



## Original Paper

# Experimental investigation on the cuttings formation process and its relationship with cutting force in single PDC cutter tests



Xian-Wei Dai <sup>a,\*</sup>, Zhong-Wei Huang <sup>b</sup>, Tao Huang <sup>a</sup>, Peng-Ju Chen <sup>a</sup>, Huai-Zhong Shi <sup>b</sup>, Shuang Yan <sup>c</sup>

<sup>a</sup> State Key Laboratory of Oil and Gas Reservoir Geology and Exploitation, Chengdu University of Technology, Chengdu, 610059, Sichuan, PR China

<sup>b</sup> State Key Laboratory of Petroleum Resources and Prospecting, China University of Petroleum-Beijing, Beijing, 102249, PR China

<sup>c</sup> PetroChina Southwest Oil and Gasfield Company Northeast Sichuan Gas District, PR China

## ARTICLE INFO

## Article history:

Received 22 March 2022

Received in revised form

26 October 2022

Accepted 26 October 2022

Available online 29 October 2022

Edited by Yan-Hua Sun

## Keywords:

Rock breaking

Cutting force

PDC cutter

Cuttings

## ABSTRACT

The single polycrystalline diamond compact (PDC) cutter test is widely used to investigate the mechanism of rock-breaking. The generated cuttings and cutting force are important indexes reflecting the rock failure process. However, they were treated as two separate parameters in previous publications. In this study, through a series of rock block cutting tests, the relationship between them was investigated to obtain an in-depth understanding of the formation of cuttings. In addition, to validate the standpoints obtained in the aforementioned experiments, rock sheet cutting tests were conducted and the rock failure process was monitored by a high-speed camera frame by frame. The cutting force was recorded with the same sampling rate as the camera. By this design, every sampled point of cutting force can match a picture captured by the camera, which reflects the interaction between the rock and the cutter. The results indicate that the increase in cutting depth results in a transition of rock failure modes. At shallow cutting depth, ductile failure dominates and all the cuttings are produced by the compression of the cutter. The corresponding cutting force fluctuates slightly. However, beyond the critical depth, brittle failure occurs and chunk-like cuttings appear, which leads to a sharp decrease in cutting force. After that, the generation of new surface results in a significant decrease in actual cutting depth, a parameter proposed to reflect the interaction between the rock and the cutter. Consequently, ductile failure dominates again and a slight fluctuation of cutting force can be detected. As the cutter moves to the rock, the actual cutting depth gradually increases, which results in the subsequent generation of chunk-like cuttings. It is accompanied by an obvious cutting force drop. That is, ductile failure and brittle failure, one following another, present at large cutting depth. The transition of rock failure mode can be correlated with the variation of cutting force. Based on the results of this paper, the real-time monitoring of torque may be helpful to determine the efficiency of PDC bits in the downhole.

© 2022 The Authors. Publishing services by Elsevier B.V. on behalf of KeAi Communications Co. Ltd. This is an open access article under the CC BY license (<http://creativecommons.org/licenses/by/4.0/>).

## 1. Introduction

Since being first introduced by General Electric in 1973 and put into use in the oil field in 1976, the polycrystalline diamond compact (PDC) bit has developed and progressed ever since (Warren and Sinor, 1994). Its applicability in hard rock has been greatly improved by innovations in impact resistance, PDC wear and a better understanding of vibrations (Gerbaud et al., 2006). The knowledge of rock failure modes and the interaction between the

rock and PDC cutter are key factors to further improve the rock-breaking ability of the PDC bits. However, it is an extremely complex process and is almost impossible to perform experiments under realistic field conditions (Che et al., 2017; Chen et al., 2021a). To this end, the single PDC cutter test has been widely used to investigate the rock failure mechanism (Glowka, 1989).

Many evaluation indexes have been applied to study the results of single PDC cutter scratching process in previous research. Among them, the variation of cutting force and the distribution of cuttings were the most common and effective. A large number of works about them have been done in the past. The cuttings formation process by PDC cutters can be recorded frame by frame with a high-speed camera, which reveals the characteristics of rock-breaking to

\* Corresponding author.

E-mail address: [daixw@cdu.edu.cn](mailto:daixw@cdu.edu.cn) (X.-W. Dai).

a large extent (ChengSheng and Li, 2018). Some scholars pointed out that rock failure modes translate from ductile to brittle with the increase in cutting depth. The morphology of the corresponding cuttings will change from fine powder to chunk-like (He and Xu, 2016; Liu et al., 2018a; Zhou and Lin, 2013). That is, the size of cuttings is closely associated with the rock failure modes. Meanwhile, some scholars investigated the shape of cuttings and assumed that the failure surface of the rock follows a parabolic representation. On the basis of this, they demonstrated that the process of rock fragmentation by PDC cutters has two stages: shear failure and tensile failure dominate, respectively (Hareland et al., 2009). Besides, drilling is an extremely complex process and is significantly affected by confining pressure and hydrostatic pressure. A series of experiments and simulations have been conducted to study the influence of these two factors. According to their results, the length of cuttings and mechanical specific energy (MSE) consumed increase simultaneously as the confining pressure rises from the atmosphere to 3.44 MPa. Furthermore, the formation of cuttings was defined as a “chip stacking process” under such conditions (Kaitky and Lei, 2005; Rafatian et al., 2010; Rajabov et al., 2012).

At the same time, large amounts of work on cutting force have been done as well. The average value (Alvarez Grima et al., 2015; Chen et al., 2016; Zeuch and Finger, 1985) and average peak value (Chen et al., 2021b; Cheng et al., 2019a; Su and Akcin, 2011) of cutting force were widely used to evaluate the ability of a rock resisting the breakage by PDC cutters. These two values were also used as an important index to investigate the effects of chamfer geometry, cutting depth, cutter size and back rake angles on the rock cutting efficiency (Akbari et al., 2014). Meanwhile, there are many other applications for the cutting force. Some researchers proposed that there is a strong correlation between rock failure modes and the variation trend of cutting force at different cutting depths. Results of their tests indicate that the cutting force is proportional to cutting depth in the ductile failure region. Otherwise, the relationship between them will be non-linear. The findings can be used to determine the value of critical depth (Nicodeme, 1997). Besides, some scholars proposed that the cutting force in the ductile failure region can be correlated with the uniaxial compressed strength (UCS) of rocks (Richard, 1999; Richard et al., 2012). The accuracy of this model was further proved by subsequent studies (Rostamsowlat et al., 2018). The frequency spectrum characteristics of cutting force were also studied by some researchers. They pointed out that there are no obvious peaks in the power spectrum density (PSD) distribution of the cutting force, which can be defined as a pink noise due to the randomness of rock failure process (DaiHuang and Shi, 2020; Dai et al., 2021; Peña, 2010).

These two important and intuitional evaluation indexes were treated as two separate parameters in most instances. Some scholars also tried to establish a relationship between them. Gnirk and Cheatham (1965) explored the failure modes of rocks based on the inclination of force when a single bit-tooth penetrates the rock. They proposed that the occurrence of chipping would result in fluctuation in the force. The same phenomenon was also discovered by other researchers (Larson et al., 1987). Some scholars pointed out that the formation and separation of a big chip were generally accompanied by an obvious drop in the cutting force. In contrast, the crushing in the cutting process would cause small variations of force. That is, the value of cutting force drop ( $\Delta F$ ) from peak to valley indicates the size of cuttings (Jaime, 2011; Jaime et al., 2015). However, no tangible proof has been proposed so far. At the same time, some scholars proposed inverse conclusions as well. Their studies showed that many sawtooth waveforms in the cutting force are independent of the volumetric breakage of rocks (Entacher et al., 2015; Gertsch, 2000). Peña (2010) studied the relationship

between force signals and the size of cuttings based on the MSE consumed in single PDC cutter tests. He argued that the generation of chunk-like cuttings will consume more energy, which will be reflected by the cutting force as well.

In a word, cutting force and cuttings all reflect the rock failure process. However, the relationship between them is still unclear. In this study, we calculated the value of  $\Delta F$  and the distribution of cuttings under different experimental conditions and investigated the relationship between them. Then, the rock failure process was analyzed through the combination of cuttings distribution and the fluctuation of cutting force. Besides, the rock sheet cutting experiments were conducted to validate our standpoints. The results of the present paper not only provide a better understanding of the rock failure process but also demonstrate its relationship with cutting force.

## 2. Experimental setup and materials

### 2.1. Experimental setup

As shown in Fig. 1, the single PDC cutter tests were conducted on a self-developed rock cutting facility, which has a moving speed of 1.6–230 mm per second in the cutting direction. With the help of the micrometer, the accuracy of cutting depth can be corrected to 0.001 mm. By moving lever (a), we can adjust the position of cutting grooves. Consequently, the same rock sample can be repeatedly tested to investigate the effects of different cutting parameters. Using lever (b) and a series of PDC holders with constant angles together, the back rake angles can be continually changed from  $-40^\circ$  to  $60^\circ$ . Besides, four dynamometers were installed and employed to accurately monitor the cutting force loaded on any point of the rock. They have a maximum sampling rate of 50,000 Hz to capture any information included in the cutting force. In our studies, a PDC cutter with the dimension of  $\phi 19 \text{ mm} \times 13 \text{ mm}$  was used and its wear was ignored due to the short cutting distance.

Fig. 2a shows the schematic of rock block cutting tests. Previous studies indicate that rock properties and the geometry shape of PDC cutter have few effects on rock failure mechanism (Zeuch and Finger, 1985). Meanwhile, the primary goal of this paper is to investigate the process of cuttings formation and its relationship with cutting force. Consequently, we just conducted experiments under different cutting depths ranging from 0.1 to 1.5 mm with an interval of 0.1 mm, namely, a total of 15 groups of tests were conducted. The cutting speed and the back rake angle were set as 300 mm/min and  $20^\circ$ , respectively.

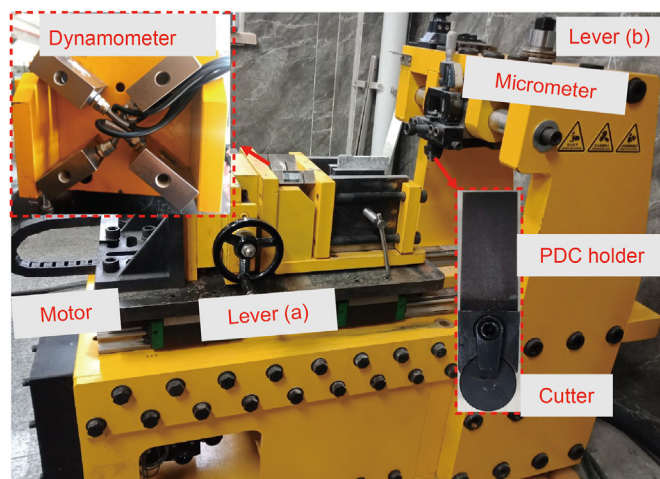


Fig. 1. The diagram of rock cutting facility.

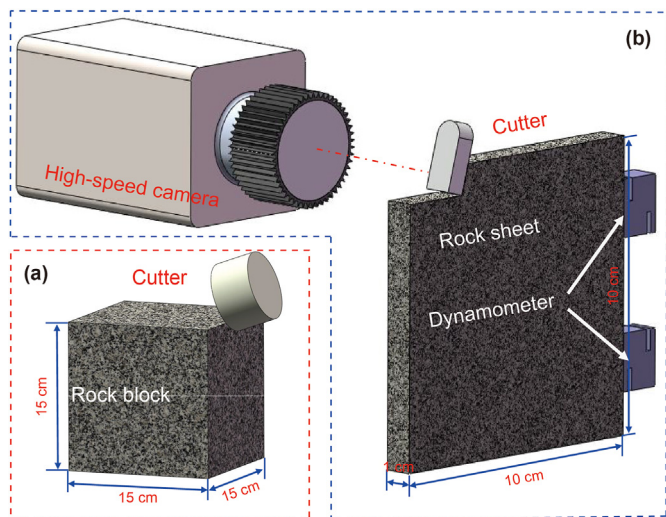


Fig. 2. The schematic of the experimental process.

The collection of cuttings plays an important role in the reliability of results. During the experiments, plastic slabs were placed along the rock to prevent the cuttings from splashing away. After each test, the cuttings were carefully brushed into a sampling bag. All things have been done were to minimize the loss and the re-crushing of cuttings in the process of collecting. After all the scratching tests were finished, the cuttings were divided into different size groups by sieves with various mesh sizes. Five groups of cuttings were produced and weighted with an electrical balance (with an accuracy of 0.001 g).

As shown in Fig. 2b, to validate the results concluded in rock block cutting tests, another experiment was conducted to directly observe the cuttings formation process and its relationship with cutting force. A high-speed camera was used to capture the characteristics of instantaneous rock failure frame by frame. Moreover, the sampling rate of both the cutting force and the high-speed camera was set as 1000 Hz. By this design, every sampled point of cutting force can be correlated with the characteristics of instantaneous rock-breaking. Besides, in our studies, the PDC cutter was fixed and the rock moved with a constant speed to conduct rock cutting tests. As a consequence, the immobile cutter was employed for the focusing of the camera, which is easier to be achieved.

### 2.2. Material

The granite with no obvious damage on the surface was chosen for our experiments. It was collected from the formation of outcropping in the Shandong Province. To meet the different demands, rock was machined into blocks and sheets, respectively. The corresponding dimension of them is shown in Fig. 2. The flatness and roughness of the rock surfaces were strictly controlled, thereby the cutting depth can be accurately adjusted. In our tests, six surfaces of the same rock block were employed to minimize the effects of rock heterogeneity on our results. Table 1 shows partial important physical and mechanical properties of rock samples.

Table 1  
Physical and mechanical properties of rock samples.

Property	Density, g/cm <sup>3</sup>	Cohesive strength, MPa	Young's Modulus, GPa	Internal friction angle, degree	Poison's ratio	UCS, MPa
Value	2.63	37.88	35.46	53.18	0.28	164.2

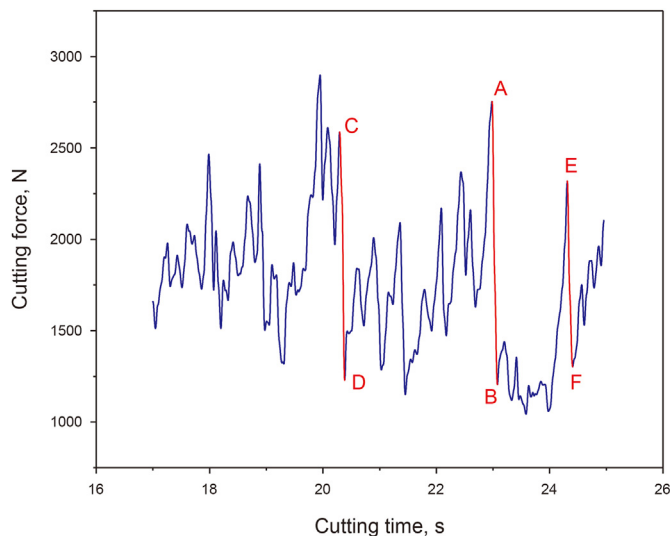


Fig. 3. The variation of cutting force.

## 3. Results and discussion

### 3.1. The variation of cutting force and the characteristics of cuttings

To explore the relationship between cutting force and cuttings formation process, the variation of these two parameters was separately studied at first. As shown in Fig. 3, the cutting force obtained in the rock block cutting tests (at the cutting depth of 1.5 mm) intensely fluctuates with time. That is, a continuous rise of force is accompanied by a subsequent drop, which includes a large amount of useful information. When the rock in front of the PDC cutter is squeezed, the cutting force increases from a valley to a peak, while the energy accumulates in this stage. When the force exerted by the PDC cutter exceeds the strength of the rock, the breakage occurs and the cutting force decreases to a valley. The value of cutting force drop ( $\Delta F$ ) from peak to valley (as the red line shows) distributes within a wide range, which includes valuable information. In Fig. 3, from A to B the  $\Delta F$  is the largest, followed by CD and EF.

To reveal the potential information included in the cutting force, the value of  $\Delta F$  at different cutting depths is calculated and arranged in ascending order. As shown in Fig. 4, an overall increase in the maximum  $\Delta F$  at a larger cutting depth can be detected. In the rock cutting tests, the energy is accumulated in the loading process and released in the failure process. That is, the accumulated energy is used for producing new surfaces of cuttings. It is obvious that the area of cuttings is proportional to its size. As a result, the generation of larger size of cuttings needs to consume more energy based on the theory of specific surface energy (Carpinteri and Pugno, 2002; Rabia, 1982). And the  $\Delta F$  that corresponds to the bigger size of cuttings will become larger in the rock failure process.

At the same time, the generated cuttings in our experiments are sieved with four different mesh screens: 10 mesh (2 mm), 20 mesh (1 mm), 40 mesh (0.45 mm) and 80 mesh (0.18 mm). The mass fraction is used to evaluate the distribution of cuttings with different sizes, which is expressed as follows:



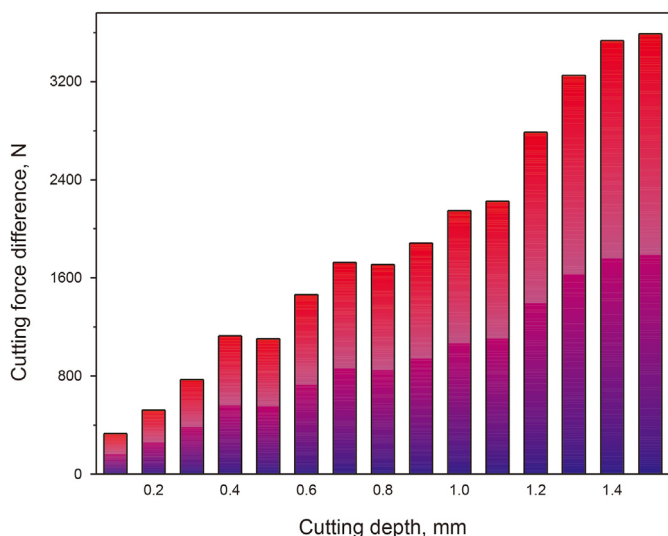


Fig. 4. The distribution of  $\Delta F$  at different cutting depths.

$$w = \frac{m_i}{\sum m_i} \times 100\% \tag{1}$$

where  $m_i$  is the mass of cuttings in every group.

As we can see in Fig. 5, the mass fraction of the powdery cuttings (>80 mesh) becomes lower with the increase in cutting depth. Especially as the cutting depth is smaller than 0.6 mm, an almost linear decrease in powdery cuttings can be observed. Meanwhile, the mass fraction of chunk-like cuttings (<10 mesh) shows an obvious increasing trend as the cutting depth becomes larger, which is consistent with the variation of the maximum  $\Delta F$  shown in Fig. 4. It seems that the increase in the  $\Delta F$  leads to an increase in the size of cuttings. In other words, the cuttings with large sizes would not generate until the  $\Delta F$  beyond a specific value. The association of cutting force drops with rock failure was also proposed by other researchers (Entacher et al., 2015; Gnirk and Cheatham, 1965; Larson et al., 1987). However, no subsequent proofs were proposed to validate this standpoint.

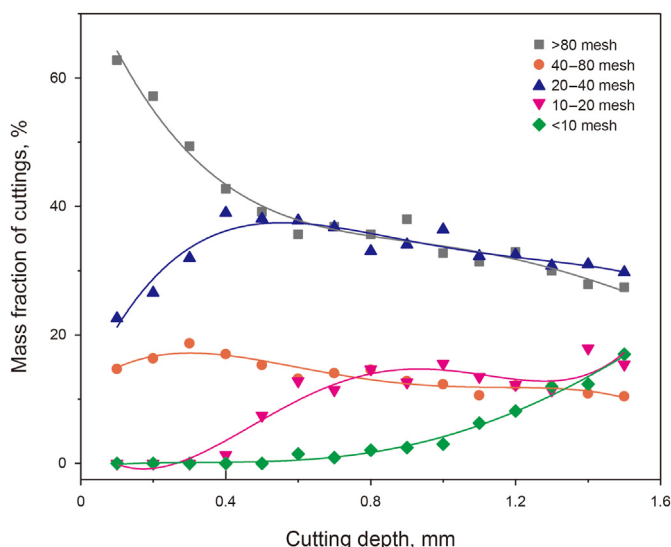


Fig. 5. Mass fraction of cuttings at different cutting depths.

To prove the relationship between them, the cuttings formation process is investigated firstly. At shallow cutting depths, the volume of rocks in front of the cutter is small, which is easy to be broken. Therefore, ductile failure dominates, which has been manifested by other scholars (He and Xu, 2016; He et al., 2017; Huang et al., 2013; Liu et al., 2018a, 2018b; Zhou and Lin, 2013). The energy is continually accumulated and released and the corresponding  $\Delta F$  cannot reach a great value.

With the further increase in cutting depth, brittle failure dominates and chunk-like cuttings appears, whose topography is shown in Fig. 6. Among them, the back of cuttings has a coarse surface, its corresponding height along the axis of AC is shown in Fig. 7a. The results indicate that cracks initiate from a specific depth and propagate to the free surface of the rock. The rock cutting direction and the edge that contacts the PDC cutter can be easily determined as well.

Besides, the maximum thickness of cuttings appears in point B rather than point C. That is, cracks tend to expand into the rock in the initial stage of cuttings formation. As shown in Fig. 7b, the distribution of Mises stress ahead of the cutter shows arc-shaped in the rock cutting process, which presents a great resemblance to the profile of cuttings (Zhao et al., 2021). Consequently, shear failure controls the initiation of cracks in the rock failure process. Similar results were also concluded by other scholars (Alvarez Grima et al., 2015; Cheng et al., 2019a).

The front of cuttings includes a flat surface and a crushed zone. Among them, the former is the original surface of the rock, while the crushed zone is mainly affected by the last rock failure process. Due to the existence of this region, the actual cutting depth decreases significantly. Depending on the rock cutting direction and the topography of cuttings, we can get a clear understanding of chunk-like cuttings generation. That is, when the PDC cutter contacts and squeezes the rock, the energy is accumulated to initiate the crack to the free surface of the rock. The produced cuttings splash away with a high velocity, thereby resulting in a clearance between the rock and PDC cutter. This process is accompanied by a significant decrease in cutting force. Moreover, it is hard to accumulate energy again in a short time because of the decrease in actual cutting depth. The generation of each cuttings with a large size is an independent process and is well reflected by the cutting force.

Meanwhile, the results shown in Fig. 5 indicate that powdery cuttings still exist at great cutting depth. Based on the rock failure mechanism, the appearance of the relatively small size cuttings at this moment mainly has three reasons. At first, when the depth of cut is beyond the critical depth, the cuttings will be removed in the brittle failure mode. The energy is needed for the initiation and propagation of cracks in this process. Therefore, the rock ahead of

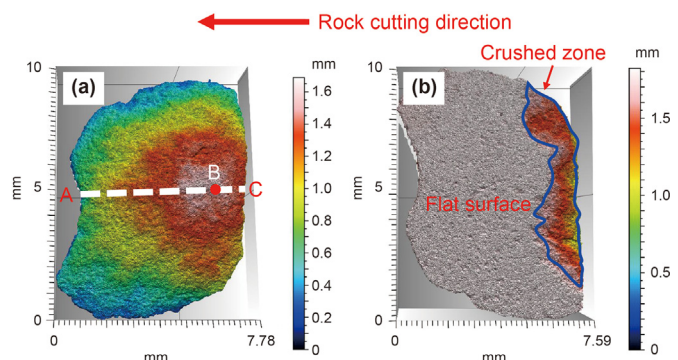


Fig. 6. The topography of back (a) and front (b) of the chunk-like cuttings.

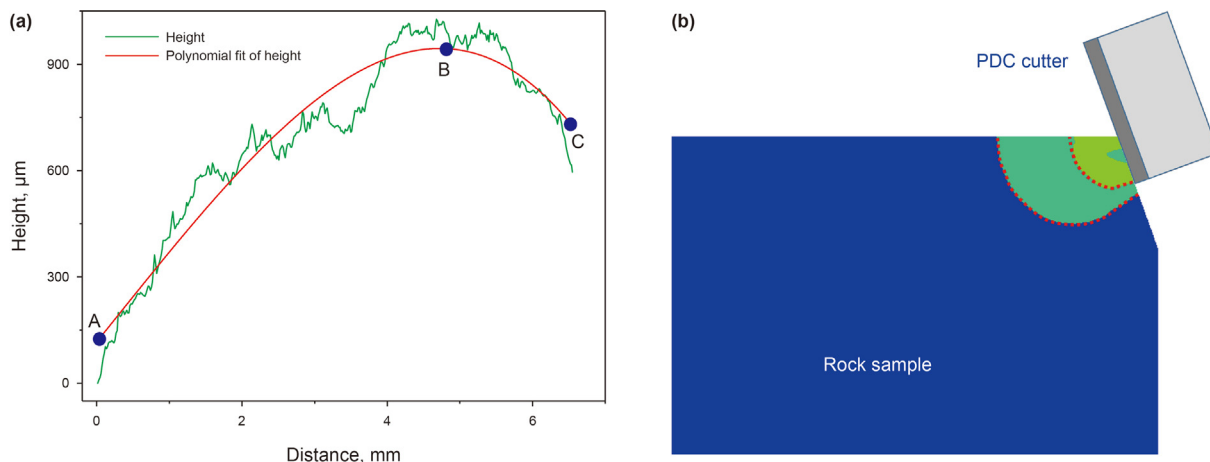


Fig. 7. The distribution of cuttings height (a) and the Mises stress ahead of the cutter (b).

the PDC cutter will be compressed and broken by crushing, which is used for accumulating energy. As shown in the area ① in Fig. 8, there is a crushing zone in front of the PDC cutter and cuttings with small size generates. This zone has been proposed and proved by many researchers (Cheng et al., 2019b). That is, the generation of chunk-like cuttings is accompanied by many small-size cuttings. Furthermore, some researchers have proved that most of the energy (more than 90 percent) is consumed to initiate the crack in this process (Larson et al., 1987).

Secondly, the volumetric breakage of the rock will generate a new surface, whose shape is linear or a curved line based on previous studies (Chen et al., 2016; ChengSheng and Li, 2018). After that, when the PDC cutter continues to move along the cutting path to remove the rock, the actual cutting depth changes and gradually increases to the pre-set value. As shown in Fig. 8, the red line is the new surface after the occurrence of brittle failure (area ② shown in Fig. 8). Then, the actual cutting depth, an important parameter that represents the real contact depth between the rock and the cutter decreases to a small value. As discussed easier, rock is broken by crushing at shallow cutting depth (area ③ shown in Fig. 8), thereby the small size cutting generates. Meanwhile, brittle failure will dominate again after the actual depth of cut increases to a critical value. And then chunk-like cuttings generates (area ④ shown in Fig. 8) and a new surface appears, which is accompanied by the

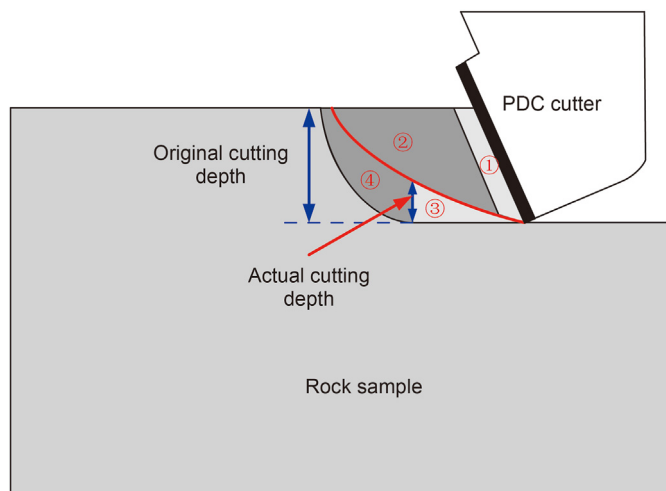


Fig. 8. The schematic of rock failure process.

subsequent ductile failure. In other words, at large cutting depths, the failure mode of the rock and actual cutting depth keep changing in the rock cutting process. The crushed zone found in Fig. 6b validates this result very well.

The aforementioned two reasons for the generation of cuttings with small sizes at great cutting depth could also be well reflected by the variation of cutting force. As shown in Fig. 9a, generally there are some fluctuations in the rock loading process, which represents the breakage of the rock. However, the same phenomenon is hardly found in the process of rock failure. Therefore, we can sure that these fluctuations are not resulted by the data acquisition system error. It is shown that the cutting force will continue to increase to its peak value after a small decrease, and then a big value of  $\Delta F$  appears. The process of rock loaded is thought to be continuous and these fluctuations are the sign of rock failure with compression, which is used to accumulate energy for the initiation and propagation of cracks.

At the same time, the generation of small-size cuttings due to the change of actual cutting depth also has significant effects on the variation of cutting force. As we can see in Fig. 9b, a big value of  $\Delta F$  appears in the rock failure process (from point A to point B), which means the occurrence of volumetric breakage and the generation of chunk-like cuttings. After that, the cutting force fluctuates in a small range and cuttings with small size appears due to the decrease in actual cutting depth (from point B to point C). When the actual cutting depth increases to a threshold value, brittle failure dominates and the value of  $\Delta F$  increases to a relatively great value (from point C to point D). Afterwards, the variation of cutting force maintains within a small range until the actual cutting depth is beyond the critical depth again (from point E to point F). Furthermore, a general increasing trend of cutting time between the two adjacent peak values is observed as the value of  $\Delta F$  increases. That is, the increase in the volume of rock failure leads to an increase in the time to form the next volume breakage.

The third reason for the generation of small-size cuttings can be concluded from Fig. 7a. The edge of the cuttings has a small thickness, which results in its low strength. In the rock failure process, there will be a large number of cuttings fragments and then generates cuttings with a small size.

### 3.2. The visualization of cuttings formation process

Based on previous research and the results in the present study, ductile failure dominates at shallow cutting depths (Che et al., 2017; ChengSheng and Li, 2018). Consequently, only small-size cuttings

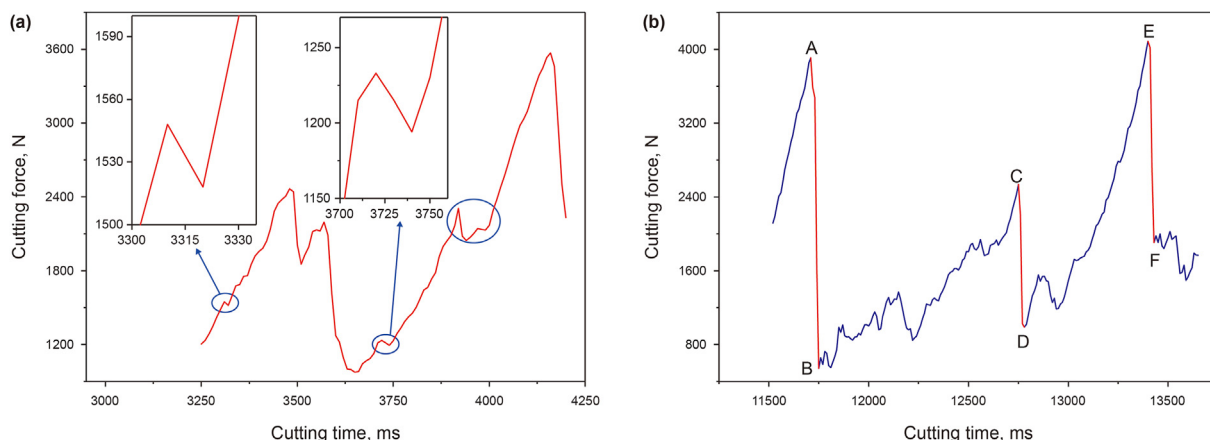


Fig. 9. The variation of cutting force due to energy accumulation (a) and the change of cutting depth (b).

generates and the cutting force fluctuates slightly. This is a clear process and no further proof is needed. However, the cuttings distribute in a wide range and the cutting force fluctuates drastically with the increase in cutting depth. Moreover, these two parameters can be correlated to each other to obtain an in-depth understanding of rock-breaking process and the interaction between the rock and cutter.

To validate the rock failure process and its relationship with cutting force at great cutting depth, the cutting force is monitored and the corresponding rock-breaking process is recorded when cutting the rock sheet. The depth of cut was set as 1.5 mm and the back rake angle is equal to 20°, which is consistent with rock block cutting tests.

Firstly, some specific points are used to determine the corresponding moment between the cutting force and rock failure process. One is the time that rock cutting started. At this point, the clearance between the rock and the cutter decreases to zero and the corresponding cutting force begins to increase. Besides, it is relatively easy to determine the time that the first volumetric breaking of the rock occurs. At this moment, the cutting force reaches the peak value and follows a significant drop, while the splashing of cuttings is also an obvious phenomenon and easy to be captured by the camera. With these points, we can unify the timeline and determine the one-to-one correspondence between the cutting force and characteristics of instantaneous rock-breaking.

As shown in Fig. 10, the cutting force shows a resemble variation trend with that in Fig. 3. At point A, the PDC cutter contacts with the rock, and the cutting force gradually increases. In the loading process, some slight drops of cutting force can be observed. At point

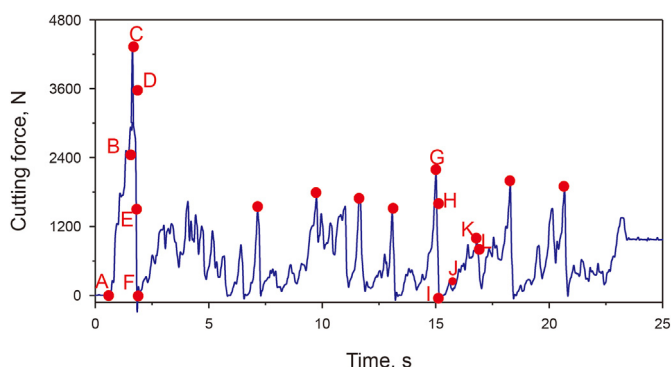


Fig. 10. The variation of cutting force.

C, the first obvious peak value is obtained. Then, the cutting force decreases to the valley with a higher speed compared with the rock loading process. Based on the analysis shown in Section 3.1, rock cutting process is accompanied by the variation of actual cutting depth. Meanwhile, an arc-shaped surface generates after the occurrence of chipping (as shown in Fig. 8). The area of rock that contacts with the cutter and cutting depth reaches the maximum values at initial conditions. Thereby, the cutting force at point C is far larger than the average value. Besides, the variation of cutting force shows great periodicity. That is, slight fluctuations occur frequently between two significant cutting force drops. In our studies, limited by the memory space of the high-speed camera, the cutting distance is smaller than the length of rock. Consequently, when the cutting process is over, the interaction between the rock and the cutter still exists and the cutting force maintains a constant value rather than decreases to zero.

Meanwhile, the characteristics of rock breaking at different times are analyzed frame by frame. Firstly, some specific points in the first loading and failure process of the rock have been selected (from point A to point F in Fig. 10) and the corresponding instantaneous rock breaking is shown in Fig. 11. At 0.668 s, the cutter contacts with the rock and loading process begins. At 1.363 s, the splashing of cuttings and a small area of crushing ahead of the cutter can be detected, which corresponds to point B in Fig. 10. The cutting force decreases slightly at this point. This validates the rock crushing when accumulating the energy for the crack initiation. In this process, the failure of the rock has few effects on the complete contact between the rock and the cutter. Thereby, just a soft fluctuation is found in the cutting force. As time goes on, the cutting force reaches its maximum value at point C. The corresponding characteristic of rock failure is shown in Fig. 11c. At this moment, the crushing zone increases significantly and the energy is sufficient for the initiation of cracks. When the cutting time increases to 1.698 and 1.749 s (the corresponding point of D and E in Fig. 10), volumetric breaking of the rock occurs and accompanies by a sharp decrease in cutting force. Meanwhile, a great number of small-size cuttings generates, which is produced by the compression of PDC cutter and used for the accumulation of energy. After that, the cutting force decreases to a valley (point F), and an obvious new surface can be found ahead of the cutter in Fig. 11f, which results in a small actual cutting depth in the subsequent rock cutting process.

Besides, to validate the reason for the slight fluctuation of cutting force after its big drop, a series of points are selected (from point G to point L) and the corresponding rock failure characteristics are shown in Fig. 12. At 15.007 s, the crushed zone appears and expands ahead of the cutter, while the cutting force reaches a



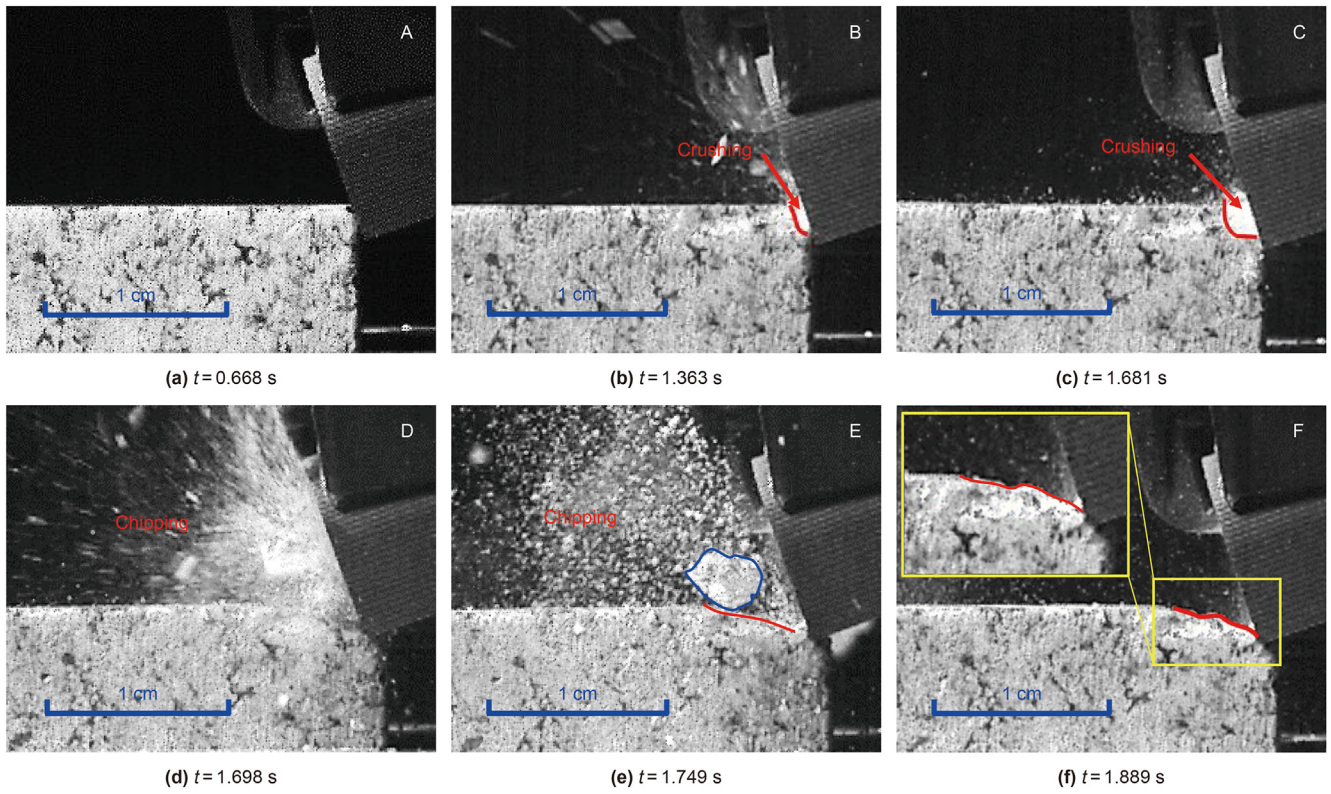


Fig. 11. The whole process of rock loading and rock breaking.

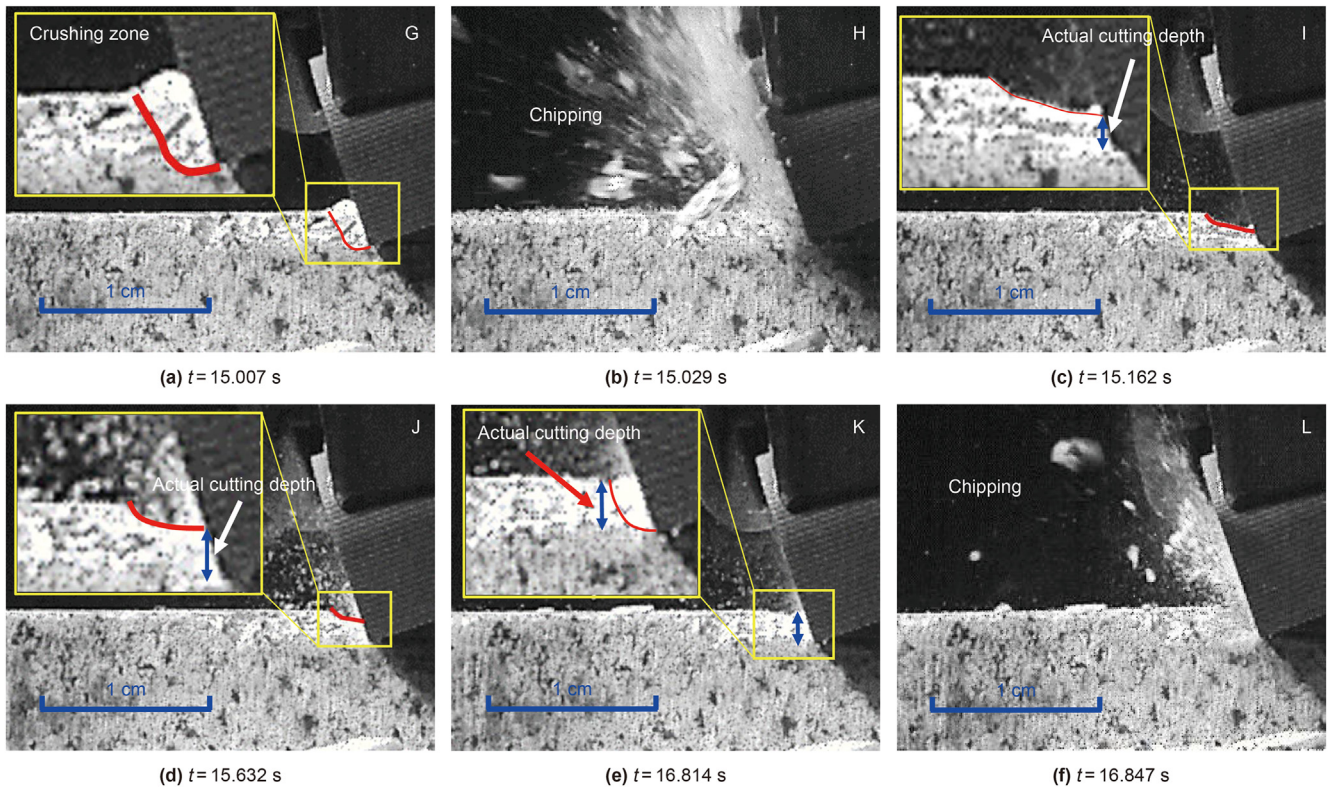


Fig. 12. Rock failure process under different cutting depths.

peak value as well (point G in Fig. 10). Just like the aforementioned result, the subsequent chipping happens at 15.029 s, and the cutting force decreases to the valley quickly (point H). Then, at point I, the actual depth of cut decreases to a small value at 15.162 s and the arc-shaped new surface can be discovered. With the rotary of the motor, the rock gradually moves to the cutter. In this stage, the actual cutting depth is small and ductile failure dominates. From point I to point K, the cutting force always fluctuates slightly. We can see that only the cuttings with a small size generates at 15.632 s (point J in Fig. 10). This phenomenon also presents the rock failure process at shallow cutting depth and its correlation with cutting force. With further movement of the rock, the actual cutting depth exceeds the critical value and brittle failure dominates, thereby the chipping occurs again at 16.847 s, and the amplitude of cutting force drops increases.

Based on the results, the fluctuation of cutting force can be correlated with the generation of cuttings and the failure mode of the rock. Meanwhile, an in-depth understanding of the cuttings formation process at different cutting depths is obtained. That is, at shallow cutting depth, only the ductile failure dominates and the cutting force fluctuates slightly. However, with the further increase in cutting depth, brittle failure and ductile failure alternatively present, thereby large cutting force drops occur regularly as well.

#### 4. Conclusions

In the present study, a series of single PDC cutter tests were conducted to investigate the process of cuttings formation and its relationship with cutting force. After each test, the cuttings lying within the window was carefully collected and sieved into different sizes with several screens. Meanwhile, the rock sheet cutting tests were performed and this process was recorded with a high-speed camera to validate our standpoints. By analyzing the distribution of cuttings and the variation of cutting force, we mainly summarized the conclusions as follows. At shallow cutting depth, ductile failure dominates, thereby only the powdery cuttings generates. Beyond the critical depth of cut, brittle failure can be detected. Cuttings is produced by the propagation of cracks and the corresponding size increases significantly. However, there are large numbers of cuttings with small size arises as well. Based on the mechanism of rock breaking and topography of chunk-like cuttings, three reasons result in this phenomenon: the change of actual cutting depth, the re-crushing of large-size cuttings and the process of energy accumulation. The generation of cuttings under different conditions can be well reflected by the variation of cutting force. Besides, the volume of cuttings has a strong correlation with the amplitude of cutting force drops. Obviously, as a result of the heterogeneity of the rock and the relatively stochastic process of rock failure, there is not an exact one-to-one correspondence between the  $\Delta F$  and cuttings. However, the value of  $\Delta F$  can be used to determine the size of cuttings to a large extent based on our experimental results. Thereby, in the drilling process, the variation of the torque that monitored on the ground can be employed to analyze the efficiency of PDC bits in the downhole. Through the analysis of this paper, a clear understanding of the rock failure process is obtained and its relationship with cutting force becomes more distinct.

#### Acknowledgments

Authors would like to acknowledge the financial support from the National Natural Science Foundation of China (52204004) and the National Science Fund for Distinguished Young Scholars (51725404) and their approval of publishing this paper.

#### References

- Akbari, B., Miska, S.Z., Yu, M., Rahmani, R., 2014. The Effects of Size, Chamfer Geometry, and Back Rake Angle on Frictional Response of PDC Cutters. 48th U.S. Rock Mechanics/Geomechanics Symposium. American Rock Mechanics Association.
- Alvarez Grima, M., Miedema, S.A., van de Ketterij, R.G., Yenigül, N.B., van Rhee, C., 2015. Effect of high hyperbaric pressure on rock cutting process. *Eng. Geol.* 196, 24–36. <https://doi.org/10.1016/j.enggeo.2015.06.016>.
- Carpinteri, A., Pugno, N., 2002. A fractal comminution approach to evaluate the drilling energy dissipation. *Int. J. Numer. Anal. Methods GeoMech.* 26 (5), 499–513. <https://doi.org/10.1002/nag.209>.
- Che, D., Zhang, W., Ehmann, K., 2017. Chip formation and force responses in linear rock cutting: an experimental study. *Journal of Manufacturing Science and Engineering-Transactions of the ASME* 139 (1). <https://doi.org/10.1115/1.4033905>.
- Chen, P., Miska, S., Yu, M., Ozbayoglu, E., 2021a. Modeling of cutting rock: from PDC cutter to PDC bit—modeling of PDC bit. *SPE J.* 26 (6), 3465–3487. <https://doi.org/10.2118/206725-PA>.
- Chen, P., Miska, S., Yu, M., Ozbayoglu, E., 2021b. Modeling of cutting rock: from PDC cutter to PDC bit—modeling of PDC cutter. *SPE J.* 26 (6), 3444–3464. <https://doi.org/10.2118/205342-PA>.
- Chen, S., Grosz, G., Anderle, S., Arfele, R., Xun, K., 2016. The role of rock-chip removals and cutting-area shapes in polycrystalline-diamond-compact-bit design optimization. *SPE Drill. & Compl.* 30 (4), 334–347. <https://doi.org/10.2118/171833-PA>.
- Cheng, Z., et al., 2019a. Analytical modelling of rock cutting force and failure surface in linear cutting test by single PDC cutter. *J. Petrol. Sci. Eng.* 177, 306–316. <https://doi.org/10.1016/j.petrol.2018.09.023>.
- Cheng, Z., et al., 2019b. Cracks imaging in linear cutting tests with a PDC cutter: characteristics and development sequence of cracks in the rock. *J. Petrol. Sci. Eng.* 179, 1151–1158. <https://doi.org/10.1016/j.petrol.2019.04.053>.
- Cheng, Z., Sheng, M., Li, G., et al., 2018. Imaging the formation process of cuttings: characteristics of cuttings and mechanical specific energy in single PDC cutter tests. *J. Petrol. Sci. Eng.* 171, 854–862. <https://doi.org/10.1016/j.petrol.2018.07.083>.
- Dai, X., Huang, Z., Shi, H., et al., 2020. Rock failure analysis based on the cutting force in the single PDC cutter tests. *J. Petrol. Sci. Eng.* 194, 107339. <https://doi.org/10.1016/j.petrol.2020.107339>.
- Dai, X., Huang, Z., Shi, H., Wu, X., Xiong, C., 2021. Cutting force as an index to identify the ductile-brittle failure modes in rock cutting. *Int. J. Rock Mech. Min. Sci.* 146, 104834. <https://doi.org/10.1016/j.ijrmms.2021.104834>.
- Entacher, M., Schuller, E., Galler, R., 2015. Rock failure and crack propagation beneath disc cutters. *Rock Mech. Rock Eng.* 48 (4), 1559–1572. <https://doi.org/10.1007/s00603-014-0661-2>.
- Gerbaud, L., Menand, S., Sellami, H., 2006. PDC Bits: all comes from the cutter/rock interaction. In: IADC/SPE Drilling Conference. Society of Petroleum Engineers. <https://doi.org/10.2118/98988-MS>.
- Gertsch, R.E., 2000. Rock Toughness and Disc Cutting. Ph.D Dissertation. University of Missouri.
- Glowka, D.A., 1989. Use of single-cutter data in the analysis of PDC bit designs: Part 1 - development of a PDC cutting force model. *J. Petrol. Technol.* 41 (8), 797–849. <https://doi.org/10.2118/15619-PA>.
- Gnirk, P.F., Cheatham Jr., J.B., 1965. An experimental study of single bit-tooth penetration into dry rock at confining pressures 0 to 5,000 psi. *SPE J.* 5 (2), 117–130. <https://doi.org/10.2118/1051-PA>.
- Hareland, G., Nygaard, R., Yan, W., Wise, J.L., 2009. Cutting efficiency of a single PDC cutter on hard rock. *PETSOC-09-06-60* 48 (6), 60–65. <https://doi.org/10.2118/09-06-60>.
- He, X., Xu, C., 2016. Specific energy as an index to identify the critical failure mode transition depth in rock cutting. *Rock Mech. Rock Eng.* 49 (4), 1461–1478. <https://doi.org/10.1007/s00603-015-0819-6>.
- He, X., Xu, C., Peng, K., Huang, G., 2017. On the critical failure mode transition depth for rock cutting with different back rake angles. *Tunn. Undergr. Space Technol.* 63, 95–105. <https://doi.org/10.1016/j.tust.2016.12.012>.
- Huang, H.-y., Lecampion, B., Detournay, E., 2013. Discrete element modeling of tool-rock interaction I: rock cutting. *Int. J. Numer. Anal. Methods GeoMech.* 37 (13), 1913–1929. <https://doi.org/10.1002/nag.2113>.
- Jaime, M.C., 2011. Numerical Modeling of Rock Cutting and its Associated Fragmentation Process Using the Finite Element Method. Ph.D Dissertation. University of Pittsburgh.
- Jaime, M.C., Zhou, Y., Lin, J.-S., Gamwo, I.K., 2015. Finite element modeling of rock cutting and its fragmentation process. *Int. J. Rock Mech. Min. Sci.* 80, 137–146. <https://doi.org/10.1016/j.ijrmms.2015.09.004>.
- Kaitkay, P., Lei, S., 2005. Experimental study of rock cutting under external hydrostatic pressure. *J. Mater. Process. Technol.* 159 (2), 206–213. <https://doi.org/10.1016/j.jmatprotec.2004.04.418>.
- Larson, D.A., Morrell, R.J., Mades, J.F., 1987. An Investigation of Crack Propagation with a Wedge Indenter to Improve Rock Fragmentation Efficiency. Bureau of Mines Report of Investigations.
- Liu, W., Zhu, X., Jing, J., 2018a. The analysis of ductile-brittle failure mode transition in rock cutting. *J. Petrol. Sci. Eng.* 163, 311–319. <https://doi.org/10.1016/j.petrol.2017.12.067>.
- Liu, W., Zhu, X., Zhou, Y., Liu, Q., Wahab, M.A., 2018b. The rock failure behavior



- analysis in rock cutting using finite element analysis. In: International Conference on Numerical Modelling in Engineering. Springer, pp. 143–149. [https://doi.org/10.1007/978-981-13-2405-5\\_12](https://doi.org/10.1007/978-981-13-2405-5_12).
- Nicodeme, P., 1997. Transition between Ductile and Brittle Mode in Rock Cutting. Rapport de stage d'Option Scientifique, Ecole Polytechnique.
- Peña, C., 2010. An Experimental Study of the Fragmentation Process in Rock Cutting. M.S. Thesis. University of Minnesota.
- Rabia, H., 1982. Specific energy as a criterion for drill performance prediction. Journal of Rock Mechanics and Mining Sciences & Geomechanics Abstracts 19, 39–42. [https://doi.org/10.1016/0148-9062\(82\)90709-4](https://doi.org/10.1016/0148-9062(82)90709-4).
- Rafatian, N., et al., 2010. Experimental study of MSE of a single PDC cutter interacting with rock under simulated pressurized conditions. SPE Drill. & Cpmpl. 25 (1), 10–18. <https://doi.org/10.2118/119302-PA>.
- Rajabov, V., Miska, S.Z., Mortimer, L., Yu, M., Ozbayoglu, M.E., 2012. The effects of back rake and side rake angles on mechanical specific energy of single PDC cutters with selected rocks at varying depth of cuts and confining pressures. In: IADC/SPE Drilling Conference and Exhibition. Society of Petroleum Engineers. <https://doi.org/10.2118/151406-MS>.
- Richard, T., 1999. Determination of Rock Strength from Cutting Tests. M.S. Thesis. University of Minnesota.
- Richard, T., Dagrain, F., Poyol, E., Detournay, E., 2012. Rock strength determination from scratch tests. Eng. Geol. 147, 91–100. <https://doi.org/10.1016/j.enggeo.2012.07.011>.
- Rostamsowlat, I., Richard, T., Evans, B., 2018. An experimental study of the effect of back rake angle in rock cutting. Int. J. Rock Mech. Min. Sci. 107, 224–232. <https://doi.org/10.1016/j.ijrmms.2018.04.046>.
- Su, O., Akcin, N.A., 2011. Numerical simulation of rock cutting using the discrete element method. Int. J. Rock Mech. Min. Sci. 48 (3), 434–442. <https://doi.org/10.1016/j.ijrmms.2010.08.012>.
- Warren, T.M., Sinor, L.A., 1994. PDC bits: what's needed to meet tomorrow's challenge. In: University of Tulsa Centennial Petroleum Engineering Symposium. Society of Petroleum Engineers. <https://doi.org/10.2118/27978-MS>.
- Zeuch, D., Finger, J., 1985. Rock breakage mechanisms with a PDC cutter. In: SPE Annual Technical Conference and Exhibition. Society of Petroleum Engineers. <https://doi.org/10.2118/14219-MS>.
- Zhao, Y., et al., 2021. The rock breaking mechanism analysis of axial ultra-high frequency vibration assisted drilling by single PDC cutter. J. Petrol. Sci. Eng. 205, 108859. <https://doi.org/10.1016/j.petrol.2021.108859>.
- Zhou, Y., Lin, J.-S., 2013. On the critical failure mode transition depth for rock cutting. Int. J. Rock Mech. Min. Sci. 62, 131–137. <https://doi.org/10.1016/j.ijrmms.2013.05.004>.